

Control of Uncertain Structures Using an H_∞ Power Flow Approach

Douglas G. MacMartin and Steven R. Hall

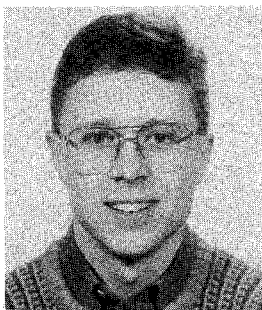
Massachusetts Institute of Technology, Cambridge, Massachusetts 02139

A technique is described for generating guaranteed stable control laws for uncertain, modally dense structures with collocated sensors and actuators. By ignoring the reverberant response created by reflections from other parts of the structure, a dereverberated mobility model can be developed that accurately models the local dynamics of the structure. This is similar in many respects to a wave-based model, but can treat more general structures, not only those that can be represented as a collection of waveguides. This model can be determined directly from transfer function data using an analysis technique based on the complex cepstrum. In order to minimize the effect of disturbances propagating through the structure, the power dissipated by the controller is maximized in an H_∞ sense. This guarantees that the controller is positive real and, thus, that the system will remain stable for any uncertainty, provided that the power flow is correctly modeled. The approach is demonstrated for two examples. The resulting controllers are much more effective than simple collocated rate feedback.

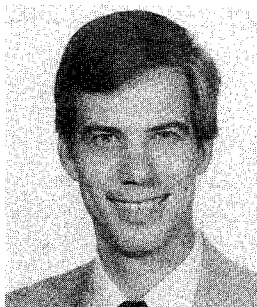
Introduction

BROADBAND active control of flexible structures is difficult for several reasons. Structures tend to be very lightly damped, modally rich, and difficult to model in detail due to their large sensitivity to parameter variations. It is well known¹ that, for many applications, there are likely to be many flexible modes within the desired bandwidth of a structural control system. This is due, in part, to the anticipated light damping, which implies that many modes can contribute to the performance, as in large space structures, where many problems of interest demand extremely precise pointing. Also, performance requirements may push the bandwidth higher directly, for example, in noise control of machinery, where the bandwidth must clearly include acoustic frequencies and, therefore, many flexible modes.

One of the problems associated with broadband control of structures is the uncertainty in the plant model. A state space model of a structure must be at best an approximation since the true structure is infinite dimensional. Finite element methods are typically used to model a structure and are sometimes capable of modeling the lowest modes quite accurately. However, in the region of high modal density, any model is likely to be highly inaccurate. Models of structures with closely spaced modes, in particular, tend to be extremely sensitive to small parameter changes in their prediction of natural frequencies and, especially, in their prediction of mode shapes. As a result, the actual structure to which the control will eventually be applied may differ significantly from the model for which it was designed. Thus, some knowledge about the uncertainty must be taken into account when designing the controllers.



Douglas MacMartin received his B.A.Sc. in Engineering Science from the University of Toronto in 1987 and his S.M. in Aeronautics and Astronautics from the Massachusetts Institute of Technology in 1990. He is currently working on his Ph.D. in the Department of Aeronautics and Astronautics at M.I.T. in active control of flexible structures. He is a student member of AIAA.

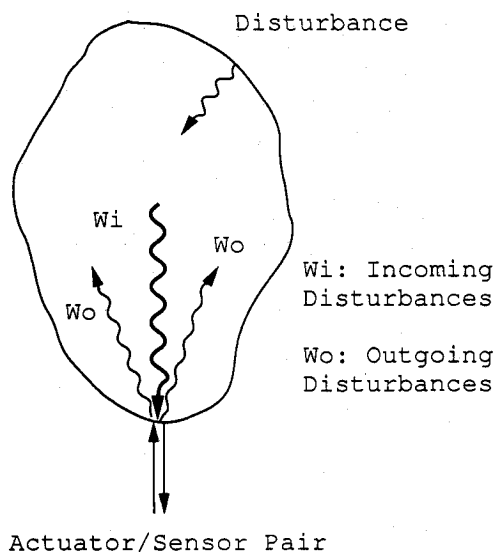


Steven R. Hall received his S.B., S.M., and Sc.D. degrees from the Massachusetts Institute of Technology, Department of Aeronautics and Astronautics, in 1980, 1982, and 1985, respectively. Since 1985, he has been with the Department of Aeronautics and Astronautics at M.I.T. His research interests include active control of flexible structures, control of helicopter and machinery vibration, and control of flight vehicles. He is a senior member of AIAA, and a member of IEEE and the American Helicopter Society.

Many approaches to control design for uncertain structures²⁻⁴ begin with a large-order, detailed nominal model of the structure and deal with uncertainty by attempting to model it, as well as the nominal plant, in some fashion. However, if the nominal model contains significant error, then the detailed information it contains is meaningless and has no effect other than to increase the computational burden associated with the control design. Indeed, for broadband control of a modally rich structure, the dimension of the plant required to model each mode may be prohibitive for many control design techniques. Instead, only the information that can be modeled accurately should be included in the description of the plant.³ With this philosophy, there has been much recent research on the use of wave-based models for use in structural control; see, for example, Refs. 5-12. Here, the assumption is that the local dynamics can be modeled accurately, and that an effective control system can be derived based only on this information.

Of particular relevance to this paper is the optimal control approach of Miller et al.⁵ The structure is represented as being composed of one-dimensional waveguides, i.e., structures that support traveling waves along a single dimension, such as beams in bending or rods in compression. These meet at junctions, and only the junction at which the control acts is modeled. Using Weiner-Hopf techniques to ensure causality, Miller et al. maximize the frequency weighted power dissipation associated with the control. The drawback to this optimization is that it will allow power to be generated at some frequencies in order to achieve greater power dissipation at other frequencies. If there is a mode of the system at such a frequency, it may be destabilized by this compensator. Although power generation may be acceptable in a frequency range where the modes are well known, it is not satisfactory if the uncertainty in modal frequency is comparable to the modal spacing. This problem is corrected by approximating the optimal compensator with a positive real form, which is guaranteed to be stabilizing. The final result, then, is suboptimal because the positive real constraint is applied in a somewhat ad hoc manner. Furthermore, arbitrary structures may be difficult to model using this approach because of the difficulty in obtaining an accurate wave description. Thus, although this design procedure is attractive, an approach that treats more general structures and provides a guarantee of stability is desired.

This paper describes a new approach to the modeling and control of uncertain structures that will guarantee both stability robustness and some amount of performance robustness. The goal is to provide broadband damping to the structure.



One approach to obtaining such a model is through the use of waves. However, it may be difficult to obtain a useful wave description for many complicated structures because not all structures can be well represented as a collection of waveguides. An alternative to a wave approach is to represent the structure by its dereverberated driving point mobility.¹⁶ The mobility is the ratio of a generalized velocity and a generalized force, which is the inverse of the mechanical impedance. The driving point mobility is then the transfer function between two variables whose product is the power flow into the structure; thus, the sensors and actuators must be both collocated and dual. The response at a point can be considered to be the sum of two parts: a direct field, due to the local dynamics; and a reverberant field, which is caused by energy reflected back from other parts of the structure. The term dereverberated implies that the reverberant part of the response has been removed before computing the mobility. It should be possible to model the direct field more easily and accurately than the reverberant field, as it depends only on a few parameters, whereas the reverberant field depends on the entire structure. For the same reason, it is the reverberant field that contains greater detail and requires more degrees of freedom to model. Thus, by using the dereverberated mobility, a lower order model can be used that is based only on the details of the structure that can be modeled accurately.

The dereverberated mobility may be calculated through the use of the cepstrum¹⁶ of the impulse response. The cepstrum is the inverse Fourier transform of the log of the complex spectrum and is a function of time. The low time portion corresponds to the direct response, and the high time portions correspond to the reverberant response, with spikes at times corresponding to the return times of the impulse from the rest of the structure. Windowing the cepstrum before the first of these yields the direct response, which can then be transformed back to the frequency domain to yield the dereverberated mobility. This approach is shown schematically in Fig. 2 for the transfer function from force to collocated velocity at one end of a free-free beam. The dereverberated mobility and cepstrum in this figure were calculated directly from the exact local model of the structure. The cepstrum of the dereverberated structure is only approximated by the truncated cepstrum of the original reverberant system.

The truncation time to choose can be based on the level of confidence in the impulse response data. This illustrates one of the differences between the dereverberated mobility and a local wave model—the direct control over how much of the structure is included in the model. By truncating the cepstrum at the appropriate point, some information about the rest of the structure is maintained while the details of it are ignored. Thus, the control design is provided with more information, which allows it to do a better job.

The fundamental distinction between this and the wave approach is the ability to treat generic structures. Although the concept of direct and reverberant fields is based on wave ideas, there is no requirement to actually identify a local wave model. All that is needed is the input/output behavior at the driving point, which may be found from experimental data, calculated from some nominal model, or found analytically, perhaps even from a wave model. This also indicates another important advantage of this modeling approach—the ability to use experimental data to generate a measurement-based model.

The effect of ignoring the reverberant field is to smooth out the transfer function. If no energy returns from beyond some closed surface surrounding the actuator, then this is equivalent to the structure beyond this surface either being infinite in extent or having perfectly absorbing boundary conditions. This has also been shown^{18,19} to be equivalent to replacing the log magnitude of the original transfer function with its mean. This is not surprising, considering that the cepstral analysis approach described earlier is essentially the same as low-pass filtering the logarithmic frequency response. Thus, another

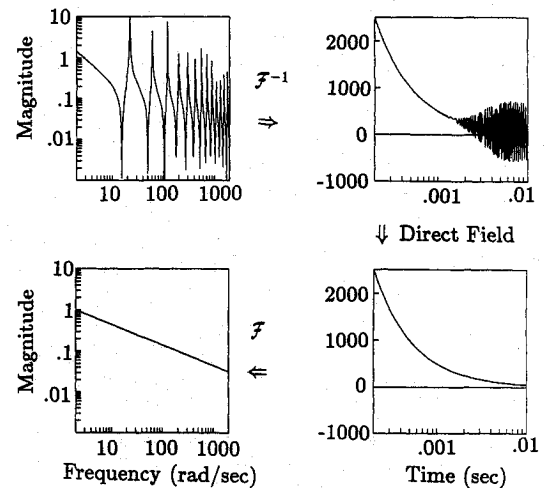


Fig. 2 Calculation of dereverberated mobility from complex cepstrum.

way to compute the dereverberated mobility is simply to take the logarithmic average of the magnitude of the transfer function, with the phase being determined uniquely from the fact that the dereverberated mobility is positive real. In practice, this method should be adequate. Fitting the result with a rational polynomial gives a model that captures the essential dynamics of the system over a wide frequency range that encompasses many modes, with only a small number of poles and zeros.

The dereverberated mobility model is not intended to represent the structure accurately. Clearly, it fails in this regard. However, it is shown in the examples that this can be a useful model for the design of control systems for the structure. Although the local dynamics of the controlled junction are modeled accurately by the dereverberated mobility, the resonant and antiresonant details of the full reverberant mobility are not explicitly modeled. However, the reverberant field is composed of waves whose behavior is governed by the local dynamics of the controlled junction each time they pass through it. Thus, if the local dynamics can be modified appropriately based on a local model, then the complete reverberant field can be controlled.

Control Design

The previous section described the modeling approach used, whereas this section focuses on the design of the control system for this model. There are two main objectives to be satisfied by the control design. It must be guaranteed to be stabilizing for all possible plants and it must provide good performance for all possible plants. In order to guarantee stability, positive real feedback from velocity to force will be required. One could, for example, select rate feedback, which is guaranteed to be stable, but this does not necessarily give the best performance that could be achieved. The object of this section is to derive the optimal positive real compensator.

The criterion to be used for optimality will be the minimum power flow into the structure. That is, power extracted from the structure will be maximized. Power flow is the appropriate quantity to minimize to provide active damping of the structure and allows a guarantee of stability by ensuring that the power flowing into the structure due to the control is always negative.

Miller et al.⁵ minimized the H_2 norm of the power flow. This required some assumptions about the power spectral density of the disturbance entering the junction, which in the actual structure is related to the control through the disturbance that previously departed the junction. In the wave model, however, it was assumed constant and independent of the control, and, thus, the resulting compensator allowed power to be added at some frequencies. This problem can be

avoided by minimizing the power flow in an H_∞ setting. For an open-loop system, the power removed by the controller is zero, and the closed loop is guaranteed to be no worse. In fact, it is sufficient to place a constraint on the maximum value of the power flow that guarantees it to be negative at all frequencies and then to use an H_2 optimization,²⁰ which may improve the overall performance.

Define $G(s)$ to be the dereverberated driving point mobility, and assume some disturbance input d to be additive at the output. Then the output y is related to the input u and the disturbance via

$$y(s) = G(s)u(s) + d(s) \quad (1)$$

As yet, no assumptions have been made about the nature of the disturbance.

The disturbance d in Eq. (1) can be thought of as originating from two sources: the original disturbance input to the real structure, and the reverberant field ignored in the modeling process. This second source will have significant power at the modal frequencies, and if the closed-loop damping is still relatively small, then in steady state this will be much larger than the physical disturbance. Thus, the disturbance spectrum in Eq. (1) consists of significant power in narrow-band but unknown frequency ranges, which are exactly the assumptions indicated in Ref. 20 as being appropriate for H_∞ minimization.

The instantaneous power flow into the structure is the product of the input $u(t)$ and the output $y(t)$ since $G(s)$ is a mobility. The average power flow can be expressed as a time integral of the instantaneous power flow,²¹ which can then be transformed into the frequency domain

$$P_{av} = \lim_{T \rightarrow \infty} \frac{1}{2T} \int_{-T}^T y(t)^T u(t) dt$$

$$= \int_0^\infty \text{tr}[\Phi_{uy}(\omega) + \Phi_{yu}(\omega)] \frac{d\omega}{2\pi} \quad (2)$$

where Φ_{uy} is the cross-spectral density of u and y . The integrand of the right side of Eq. (2) represents the steady-state, or average, power flow into the structure as a function of frequency, so that the average power flow at each frequency can be defined as

$$P(\omega) = \text{tr}[\Phi_{uy}(\omega) + \Phi_{yu}(\omega)] \quad (3)$$

The control law is assumed to be of the form

$$u(s) = -K(s)y(s) \quad (4)$$

Solving for the control in terms of the disturbance from Eq. (1) gives

$$u = -(I + KG)^{-1} Kd$$

$$= Hd \quad (5)$$

where the explicit dependence on the Laplace transform variable has been dropped. Then, the output can also be represented in terms of the disturbance as

$$y = (I + GH) d \quad (6)$$

Using these expressions for u and y , the cross-spectral density can be written as

$$\Phi_{uy} = (I + GH)\Phi_{dd}H^H \quad (7)$$

where Φ_{dd} is the power spectral density of the disturbance. The average power flow at each frequency is then

$$P(\omega) = \text{Tr}\{\Phi_{dd}[H^H(I + GH) + (I + GH)^H H]\} \quad (8)$$

Unconstrained Optimum

Before finding a compensator that minimizes the worst-case power flow, consider finding the compensator that minimizes the power flow at each value of the Laplace transform variable s . Equation (8) is only valid on the $j\omega$ axis and must first be extended analytically to the remainder of the complex plane. The analytic continuation of the Hermitian operator is the parahermitian conjugate,²² denoted $(\cdot)^{-}$, and defined as

$$F^-(s) = F(-s)^T \quad (9)$$

With this substitution for the Hermitian, then optimizing Eq. (8) at each point in the complex plane with respect to H yields

$$H_{opt} = -(G + G^-)^{-1} \quad (10)$$

which is independent of the disturbance spectrum Φ_{dd} . This is the optimal disturbance feed-forward control law. The equivalent feedback from the velocity is related to this from Eq. (5) by

$$K = -H(I + GH)^{-1} \quad (11)$$

So finally,

$$K_{opt} = (G^-)^{-1} \quad (12)$$

This compensator extracts the maximum possible power from the structure at every frequency. This result is not new; it corresponds to the impedance matching condition found, for example, in Ref. 23. The maximum energy dissipation is obtained if the impedance of the compensator is the complex conjugate of the impedance of the load, which in this case is the rest of the structure. Also note that although Eq. (12) was obtained using the dereverberated mobility, it is also optimal for the actual structure. The dereverberated mobility accurately models the local dynamics of the structure, and the power flow is a function of only the local dynamics. Thus, the compensator that dissipates the maximum power from the dereverberated structure will also dissipate the maximum power from the actual reverberant structure.

In general, however, the compensator in Eq. (12) is non-causal and cannot be implemented. The dereverberated mobility $G(s)$ must be both stable and causal and is, therefore, right half plane analytic (RHPA). Since it is strictly positive real, it must also be minimum phase, and, thus, the optimal compensator in Eq. (12) will be left half plane analytic (LHPA). Because both the compensator and the plant are strictly positive real, then in the Nyquist plot there are no encirclements of -1 , and K must be stable for the closed-loop system to be stable. This implies that unless the dereverberated mobility is a constant, this compensator is noncausal. One case for which the dereverberated mobility is constant is that of a uniform rod in compression, for which Eq. (12) corresponds exactly to the matched termination.

Some understanding of why the optimal compensator is almost always noncausal can be found from root locus arguments. For a point λ to be on the root locus of the plant $P(s)$, the compensator $K(s)$ must satisfy $1 + P(\lambda)K(\lambda) = 0$. In order to place the structural poles far into the left half plane, the relevant plant $P(s)$ is the structural transfer function evaluated for values of the Laplace variable s far into the left half plane.

For a lightly damped structure with a large number of closely spaced poles and zeros one can divide the complex plane into three regions. Near the $j\omega$ axis, and close to the poles and zeros, the transfer function varies significantly from its maxima to its minima, and the phase varies between $+90$ and -90 deg. If one looks at the transfer function evaluated farther into the right half plane, the effect of individual poles and zeros becomes smeared out and the transfer function

approaches the smoothed or dereverberated transfer function $G(s)$. The phase of G in some frequency region will be the average phase of the original transfer function near that region.

In the left half plane, however, the structure's transfer function is not $G(s)$. To determine the phase contribution of each pole and zero, the contour to consider must now be to the left of every pole and zero, and so each phase change has opposite sign. The result is that, in the left half plane, the structural transfer function approaches $-G(-s)$. Therefore, to move the poles far into the left half plane, $K(s)$ must satisfy $1 - G(-s)K(s) = 0$ or $K(s) = 1/G(-s)$, as given in Eq. (12).

If this compensator could be implemented, all of the poles could be moved arbitrarily far into the left half plane. Instead, the best causal compensator must be found.

Causal Optimum

The wave model of Miller et al.⁵ can also be put in a form similar to that of Eq. (1), though only for structures composed of waveguides. As discussed earlier, Miller et al.⁵ performed an H_2 optimization of the power flow, which did not guarantee dissipation at all frequencies, and, thus, did not guarantee closed-loop stability. A more appropriate optimization to guarantee stability is to minimize the worst-case power dissipation, hence, a minimax optimization of the power flow into the structure. As will be shown shortly, this can be cast as an H_∞ minimization problem. In order for this to make sense, though, the disturbance input d should be normalized to provide the same amount of power available to be dissipated at each frequency. This provides the designer with complete control over the relative importance of one frequency range to another by removing any inherent frequency weighting from the problem.

With the optimal noncausal compensator derived in the previous subsection, Eq. (12), the closed-loop power flow into the structure is given by Eqs. (8) and (10) as

$$P = -\text{tr}[\Phi_{dd}(G + G^H)^{-1}] \quad (13)$$

Introduce a scaled disturbance w related to the original disturbance d via

$$d = G_0 w \quad (14)$$

Then, if the input w has unit power spectral density at a certain frequency, the optimal noncausal compensator will dissipate unit power at this frequency, provided that the transfer function G_0 is the cospectral factor of $G + G^H$, given by

$$G_0 G_0^H = G + G^H \quad (15)$$

The block diagram for this system is shown in Fig. 3, and the system [Eq. (1)] becomes

$$y(s) = G(s)u(s) + G_0(s)w(s) \quad (16)$$

Now, consider the problem of finding a causal compensator that will minimize the worst-case power flow in Eq. (3). This

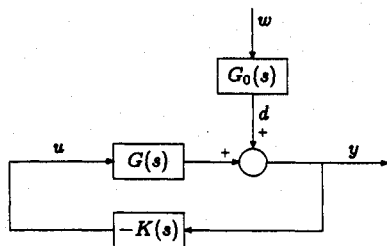


Fig. 3 System block diagram.

quantity represents the power flow into the structure, which will hopefully be negative. In order to cast this as an H_∞ optimization, however, the performance index must be positive definite. This problem can be solved by considering that the best causal compensator can dissipate no more power than the noncausal optimum. Thus, if the disturbance power $w^H w$ is added to the cost, positive definiteness will be assured.

Thus, the cost at each frequency is

$$\begin{aligned} \text{Cost}(\omega) &= w^H w + u^H y + y^H u \\ &= w^H w + u^H (Gu + G_0 w) + (Gu + G_0 w)^H u \\ &= \begin{Bmatrix} u \\ w \end{Bmatrix}^H \begin{bmatrix} G + G^H & G_0 \\ G_0^H & I \end{bmatrix} \begin{Bmatrix} u \\ w \end{Bmatrix} \\ &= |G_0^H u + w|^2 \end{aligned} \quad (17)$$

From this, we have that the relevant output that should be minimized is

$$z = G_0^H u + w \quad (18)$$

Combining this with the system equation [Eq. (16)], the result can be written as a standard problem^{24,25}:

$$\begin{Bmatrix} z \\ y \end{Bmatrix} = \begin{bmatrix} I & G_0^H \\ G_0 & G \end{bmatrix} \begin{Bmatrix} w \\ u \end{Bmatrix} \quad (19)$$

The compensator from y to u that minimizes the H_∞ norm of the transfer function from w to z will minimize the maximum power flow into the structure.

For computation, however, the unstable (1,2) block in Eq. (19) is unacceptable. Any allowable compensator must stabilize this block, whereas the only important stability constraint is on the output y . Note, however, that the norm of z is unchanged by multiplication by an inner function. An inner function is one that is stable, purely nonminimum phase, and has unit magnitude at all frequencies.²⁴ Define $\Delta(\cdot)$ to be the characteristic polynomial of the transfer function (\cdot) , and define the inner function

$$G_1(s) = \frac{\Delta[G_0^H(s)]}{\Delta[G_0(s)]} \quad (20)$$

Then redefine z to be

$$z = G_1 G_0^H u + G_1 w \quad (21)$$

so that the problem [Eq. (19)] becomes

$$\begin{Bmatrix} z \\ y \end{Bmatrix} = \begin{bmatrix} G_1 I & G_1 G_0^H \\ G_0 & G \end{bmatrix} \begin{Bmatrix} w \\ u \end{Bmatrix} \quad (22)$$

which is stable.

In general, it may be desirable to weight some frequency ranges more heavily than others while still requiring that power be removed at all frequencies. This could be because there is a known disturbance source in a certain range, because structural modes are less well damped within this range, or because the performance requirements put more emphasis on this range. Similarly, there will usually be some frequency beyond which performance is not required, and the weighting can also be chosen to reflect this.

The manner in which the weighting is introduced into the problem must be such that, if power is added to the structure somewhere, the resulting cost will be worse than the open-loop cost. Hence, rather than weighting the sum of the disturbance input power and the power input by the control, as in Eqs. (17), define the cost to be the sum of the disturbance power and some frequency-weighted control power, as

$$\text{Cost}(\omega) = w^H w + W_1^H (u^H y + y^H u) W_1 \quad (23)$$

which can be manipulated into the form

$$\text{Cost} = \left| \frac{W_1(G_0^- u + w)}{W_2 w} \right|^2 \quad (24)$$

where W_1 is the selected frequency weighting and W_2 is defined by the relationship

$$|W_1|^2 + |W_2|^2 = 1 \quad (25)$$

Note that, as desired, the open-loop cost is unity everywhere and the cost is greater than unity at any frequency where power is added to the structure. Thus, as before, a closed-loop cost of less than unity guarantees stability.

The only constraint on W_1 is that its magnitude be less than or equal to unity at all frequencies. Without this constraint, there is no guarantee that the cost will be positive definite, and the minimization could fail. Where W_1 is small, a greater amount of control effort is required to reduce the cost than before, and, thus, there is more power removed. Hence, in order to emphasize some frequency range more heavily, the weighting function W_1 should be chosen to be smaller within that region.

One of the properties of H_∞ compensators is that, at the optimum, the closed-loop transfer function being minimized is a constant function of frequency, equal to some number γ (see Ref. 24). From this, and Eq. (23), the closed-loop power absorbed by the compensator can be related to γ and the weighting function as

$$P(\omega) = \frac{1 - \gamma^2}{|W_1|^2} \quad (26)$$

This provides some insight into how to select W_1 .

The cost in Eqs. (17) or (23) can also be modified to include a penalty $\rho u^T u$ on the control effort. The problem [Eq. (22)] is modified to include an additional output in the vector z , corresponding to $\sqrt{\rho}u$. This allows a tradeoff between performance and control and also guarantees a strictly proper compensator. Similarly, it is straightforward to modify the problem [Eq. (22)] to include sensor noise. An additional disturbance input is included in the vector w , which affects only the sensor output y .

Because of the form of the cost in Eqs. (17) and (23), the final result of this approach is a compensator that dissipates power at all frequencies, provided that the optimal H_∞ cost γ is less than unity. From Eq. (7), power is dissipated provided that $[H^H(I + GH) + (I + GH)^H H]$ is negative definite. Using Eq. (11), this is equivalent to $[H^H(K^{-1} + K^{-1H})H]$ being positive definite, or $K^{-1}(j\omega) + K^{-1H}(j\omega) > 0$ for all ω . This is precisely the requirement that K^{-1} and, therefore, K be positive real.¹⁷ Hence, the approach generates a positive real compensator, which is guaranteed to be stabilizing for any positive real plant. From a mathematical perspective, the approach has replaced a phase constraint, that the compensator be positive real, with an equivalent magnitude constraint on another transfer function. The H_∞ approach guarantees satisfaction of the latter magnitude constraint and, therefore, of the original phase constraint.

If there are any time delays, actuator or sensor dynamics, or if the actuator and sensor are not truly collocated and dual, then the structure will not be positive real at all frequencies. Stability can still be guaranteed if the complementary sensitivity is bounded above by the inverse of the difference of the true structure from the positive real condition, as noted by Slater et al.¹⁷

State Space Computation

The calculation of the optimal compensator is performed most easily in state space, using the formulas given in Ref. 25. The first step, then, is to obtain a state space representation

for the plant $G(s)$ and the desired weighting function $W_1(s)$. In general, the dereverberated mobility $G(s)$ will not be rational, and a rational approximation that is valid in the frequency range of interest must be found. This approximation can also be denoted $G(s)$ without confusion since only the approximation can be used in state space calculations.

From $W_1(s)$ and $G(s)$, state space representations for $W_2(s)$, $G_0(s)$, and $G_1(s)$ must be calculated. These problems can be formulated as spectral factorization problems and solved by methods similar to those presented in Francis²⁴ or in Fuhrmann.²²

G_0 is a cospectral factor of $M = G + G^-$ and, thus, can be calculated with the standard algorithm in Ref. 24. The algorithm is restricted to systems G with a nonzero direct feed-through term D . This is not a serious restriction, however. No finite-dimensional model is valid at all frequencies, nor does it need to be. This merely implies that, rather than rolling off at high frequencies, $G(\infty)$ should be a constant.

First, define the state space representation of G as

$$G = \left[\begin{array}{c|c} A & B_2 \\ \hline C_2 & D_{22} \end{array} \right] = C_2(sI - A)^{-1}B_2 + D_{22} \quad (27)$$

The reason for the selection of the subscripts on B , C , and D is that G is the (2,2) block in Eq. (22).

G_0 can be represented as

$$G_0 = \left[\begin{array}{c|c} A & B_1 \\ \hline C_2 & D_{21} \end{array} \right] \quad (28)$$

where

$$D = D_{22} + D_{22}^T \quad (29)$$

$$A_{MT}^x = \left[\begin{array}{cc} A^T & 0 \\ 0 & -A \end{array} \right] - \left[\begin{array}{c} C_2^T \\ -B_2 \end{array} \right] D^{-1} [B_2^T \ C_2] \quad (30)$$

$$X_1 = \text{Ric}\{A_{MT}^x\} \quad (31)$$

$$B_1 = (B_2 + X_1 C_2^T) D^{-1/2} \quad (32)$$

$$D_{21} = D^{1/2} \quad (33)$$

The notation $X = \text{Ric}\{P\}$ indicates that X is the solution of the Riccati equation corresponding to the Hamiltonian matrix²⁴ P . That is, if

$$P = \left[\begin{array}{cc} A & -R \\ -Q & -A^T \end{array} \right] \quad (34)$$

then $X = \text{Ric}\{P\}$ is the positive definite solution to

$$A^T X + X A + Q - X R X = 0 \quad (35)$$

The conditions required for this spectral factorization to be valid are that $M = M^-$, which is clearly satisfied; that M and M^{-1} are proper, which is satisfied with nonzero D_{22} ; that M has no poles or zeros on the $j\omega$ axis; and that $M(\infty) > 0$. If G is dereverberated, then G has no imaginary poles and, thus, M also has no imaginary poles. The remaining conditions are satisfied if G is strictly positive real, as is the case for the dereverberated driving point mobility of any structure.

The (1,2) block in Eq. (22) is $G_1 G_0^-$. This has the stable poles, but the nonminimum phase zeros of $M = G + G^-$. This is a factorization of M , but it is not in the standard form. A modification to the standard algorithm is required, which is given in Appendix A. The result is

$$G_1(s)G_0^-(s) = \left[\begin{array}{c|c} A & B_2 \\ \hline C_1 & D_{12} \end{array} \right] \quad (36)$$

where

$$A_M^\times = \begin{bmatrix} A & 0 \\ 0 & -A^T \end{bmatrix} - \begin{bmatrix} B_2 \\ -C_2^T \end{bmatrix} D^{-1} [C_2 \ B_2^T] \quad (37)$$

$$X_2 = \text{Ric}\{-A_M^\times\} \quad (38)$$

$$C_1 = D^{-1/2}(C_2 + B_2^T X_2) \quad (39)$$

$$D_{12} = D^{1/2} \quad (40)$$

Since the remaining (1,1) block $G_1 I$ in Eq. (22) is inner, it must be true that

$$D_{11} = 1 \quad (41)$$

Then the problem in Eq. (22) is completely specified.

The computation of the weighting function W_2 in Equation (25) from W_1 can also be represented in terms of a spectral factorization. This derivation is presented in Appendix B.

Examples

Example 1: Bernoulli-Euler Beam

As an example of this approach, consider a free-free Bernoulli-Euler beam with a collocated force actuator and velocity sensor at one end. The dereverberated mobility for this system is simply that of a semi-infinite beam, which can be found, for example, from the wave approach of Ref. 5:

$$G(s) = \frac{\sqrt{2}}{(\rho A)^{1/4} (EI)^{1/4}} \cdot \frac{1}{\sqrt{s}} \quad (42)$$

For simplicity, assume the mass per unit length ρA and the bending stiffness EI are such that

$$G(s) = \frac{1}{\sqrt{s}} \quad (43)$$

This can be done without loss of generality, as it requires only a scaling of the plant.

First, consider the unconstrained optimal compensator that extracts the maximum possible energy. From Eq. (12),

$$K(s) = \sqrt{-s} \quad (44)$$

This compensator has a slope of 10 dB/decade and a phase of -45° at all frequencies. As expected, it is noncausal and cannot be implemented. Note that this is the same compensator as that obtained by the unconstrained optimization in Ref. 5, though the derivation differs, and obtained by setting the reflection coefficient to zero in von Flotow and Schäfer.⁸

Now, find the compensator that minimizes the maximum power flow into the structure. This can be done analytically; the solution is given in Ref. 14. With equal weighting at each frequency ($W_1 = 1$), the optimal causal compensator is

$$K(s) = \sqrt{s} \quad (45)$$

This is similar to the noncausal solution, Eq. (44), with the same magnitude everywhere, but a phase of $+45^\circ$ instead. This is the best causal approximation to Eq. (44) and extracts exactly half the power at all frequencies.

With velocity feedback, an appropriate choice of gain will add significant damping to a given mode, and those nearby, but it is not possible to add significant damping to all of the modes at the same time. Thus, the gain in velocity feedback must be optimized to provide damping at a certain frequency. Far enough away from this frequency, the gain is either too low to have much affect or too high so that the closed-loop poles lie near the open-loop zeros, which are undamped. With the optimal causal compensator \sqrt{s} , although no poles are

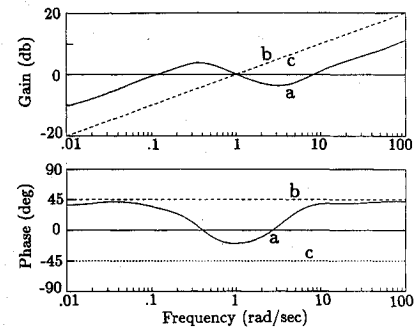


Fig. 4 Optimal compensator for example 1: a) weighting at 1 rad/s; b) no weighting; and c) unconstrained.

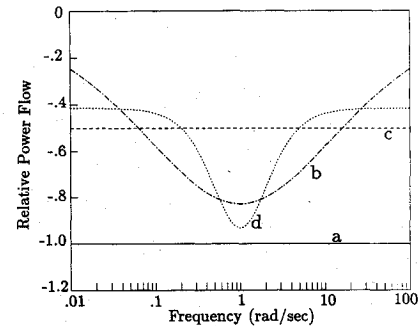


Fig. 5 Power absorption: a) unconstrained optimum; b) velocity feedback; c) unweighted H_∞ design; d) weighted H_∞ design.

damped as heavily as the best pole with velocity feedback, every pole is given some damping.

Now consider including a weighting function to increase the importance of a certain frequency range, say, in a narrow band near 1 rad/s. Select the weighting function W_1 to have poles at $1/(2\sqrt{2})$ and $2\sqrt{2}$, zeros at $(1/\sqrt{2})$ and $\sqrt{2}$, and unit magnitude far from 1 rad/s, giving it less than unit magnitude near 1 rad/s. Recall that more importance is placed where the weighting function is smaller. An analytic solution here would be difficult. However, the plant in Equation (43) can be approximated adequately over a wide frequency range with a finite number of alternating poles and zeros on the real axis with equal logarithmic spacing. The state space methods described earlier can then be used to obtain an approximate compensator. For this example, Equation (43) was approximated by 9 poles and 9 zeros on the negative real axis, between 10^{-4} and 10^4 rad/s. The transfer function of this approximation matches the exact dereverberated mobility to within 2 deg of phase and 0.25 dB magnitude for 3 decades above and below the center frequency of the weighting function.

The resulting compensator is plotted in Fig. 4, along with the optimal compensator with $W_1 = 1$ from Eq. (45) and the unconstrained optimum from Eq. (44). Far from the region that was selected as important, the compensator still has a \sqrt{s} behavior, though with a different magnitude than the unweighted optimum in Eq. (45), which will result in poorer performance. Near 1 rad/s, though, the slope of the compensator is now -10 dB/decade and the phase is closer to -45° deg. At 1 rad/s, the compensator has exactly the same magnitude and almost the same phase as the noncausal optimum and, thus, it absorbs almost all the incoming power possible. The power flow absorbed by this compensator is plotted in Fig. 5, expressed as a fraction of the available incoming power at each frequency. For comparison, the power absorbed by velocity feedback and the unweighted optimum are also plotted in the same figure.

If this control law is now applied to a finite beam, the closed-loop performance can be examined. The transfer function between force and velocity at the far (uncontrolled) end of the beam can be calculated using the phase closure ap-

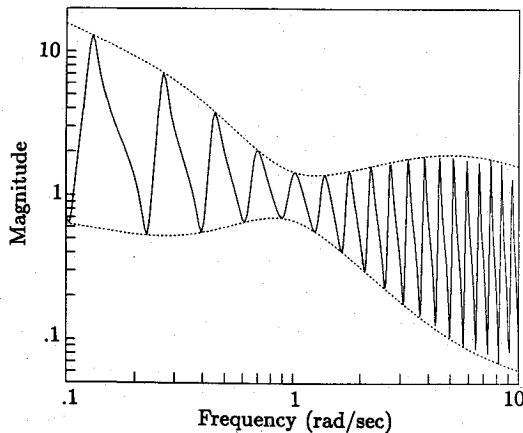


Fig. 6 Closed-loop transfer function at far end of free-free beam.

proach of Ref. 21. The beam length was chosen so that the fifth mode of the beam was at the center frequency of the weighted region. The result is plotted in Fig. 6, and the envelope of the transfer function for any length beam is also plotted. As expected, the modal peaks in the region where W_1 is smallest are more heavily damped. Note that, because the compensator in Fig. 4 is positive real, it will not destabilize the beam at any length (nor will it destabilize any positive real structure). Furthermore, the performance is insensitive to the length of the beam. For any length beam, there will be some damping achieved at all frequencies and greater damping in the region of interest, as indicated by the envelope of possible transfer functions. Also note that, although the modal information is not contained in the dereverberated mobility model of the structure, significant damping can still be added to the modes with a controller designed for this model.

Example 2: Pinned-Free Beam

As a slightly more complicated example, consider again a finite beam, but this time with one end pinned, with a moment actuator and collocated angular rate sensor at this end. Also include some finite rotational inertia J at this end. The theoretical dereverberated transfer function for this beam can be found in a straightforward manner using the wave approach of Ref. 5 to be

$$\frac{\dot{y}'}{M} = \frac{s}{\sqrt{2}(\rho A)^{1/4}(EI)^{3/4}\sqrt{s} + Js^2} \quad (46)$$

At low frequencies, the behavior is the \sqrt{s} behavior that would be the transfer function if there were no lumped rotational inertia. At high frequencies, the transfer function is dominated by the rotational inertia and rolls off at 20 dB/decade. From the far end of the beam, the controlled end then behaves as if it were clamped, and regardless of the control, all disturbances are reflected back. Thus, power flow beyond the rolloff frequency of Eq. (46) should be unimportant, and the weighting function here should be much larger than elsewhere. Also, assume again that some specific frequency range near 1 rad/s is more important.

For computation, $EI = 1/\sqrt{2}$ and $\rho A = 1/\sqrt{2}$, so that the low-frequency behavior is \sqrt{s} , and $J = 10^{-3}$ to place the rolloff frequency at 100 rad/s, at a slightly higher frequency than that considered to be important. Again, the system is approximated with a rational transfer function that is accurate over the frequency range of interest, from 10^{-4} to 10^4 rad/s.

The H_∞ and unconstrained optimal compensators for this case are shown in Fig. 7. At low frequencies, the H_∞ compensator is similar to the $1/\sqrt{s}$ that would be optimal with no rotary inertia and no weighting. Where the weighting function decreases near 1 rad/s, the phase jumps toward the unconstrained optimum phase of 45 deg and, thus, absorbs close to the maximum power possible. At high frequencies, as desired,

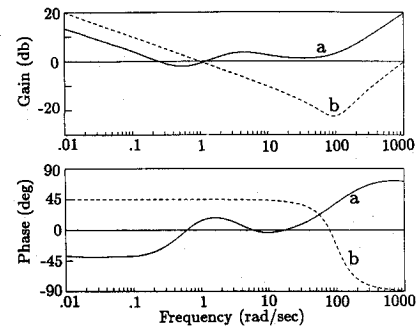


Fig. 7 Optimal compensator for example 2: a) with H_∞ design; and b) unconstrained.

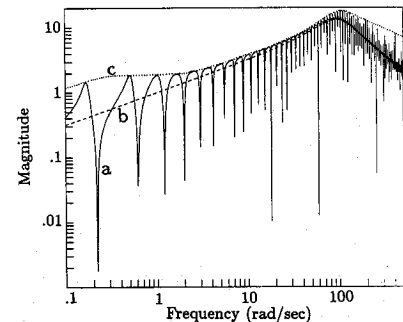


Fig. 8 a) Closed-loop transfer function at controlled end of pinned-free beam; b) dereverberated mobility; and c) envelope of possible transfer functions.

the compensator gives up and does not attempt to absorb incoming power, though it does remain positive real. Thus, again, the closed-loop system is stable for any length beam and for any boundary condition at the far end. The open- and closed-loop transfer function from moment to slope rate at the controlled end of the beam is given in Fig. 8. This transfer function shows the rolloff at 100 rad/s, beyond which the poles and zeros are essentially undamped, but almost cancel each other. The poles are more heavily damped near 1 rad/s, but none of the zeros are affected. Also plotted is the dereverberated mobility [Eq. (46)] and the upper bound of the envelope of possible transfer functions for any length of beam.

Conclusions

In this paper, an approach to broadband active damping of modally dense structures with significant uncertainty has been presented. A modal model for such a structure would be both inaccurate and unnecessarily large. Instead, the structure is modeled with its dereverberated mobility. For simple structures, this is equivalent to a local wave model and can be calculated from such a model. For general structures, the dereverberated mobility can be calculated from an experimental or analytic transfer function using cepstral analysis or by taking the logarithmic average of the transfer function. Ideally, a compensator that dissipates the most power possible at every frequency is desired. This compensator is, in general, noncausal and cannot be implemented. A causal, guaranteed stabilizing, optimal compensator can be obtained by minimizing the maximum power flow into the structure. This problem is solved by reformulating it as an equivalent H_∞ control problem. This results in a positive real controller that dissipates power at all frequencies. The importance of a certain frequency range can be increased through use of a weighting function. The technique was demonstrated for several simple examples. At the frequency deemed most important, the compensator is close to the noncausal optimum and dissipates almost all incoming power. It is expected that this approach to modeling and control design will allow significant damping to be added to many modes of a structure, without the large effort in system identification, off-line computation, and

compensator complexity that would be required of many control design techniques.

Appendix A: Modified Spectral Factorizations

A state space method is desired for calculating $G_1 G_0^-$, which has the stable poles, but the nonminimum phase zeros of $M = G + G^-$. This is related to the spectral factorization algorithm found in Ref. 24, and only the differences between the two will be indicated here.

Given G as Eq. (27), then

$$M = G + G^- = \left[\begin{array}{c|c} A & 0 \\ \hline 0 & -A^T \\ \hline C_2 & B_2^T \end{array} \middle| \begin{array}{c} B_2 \\ -C_2^T \\ D_{22} + D_{22}^T \end{array} \right] = \left[\begin{array}{c|c} A_M & B_M \\ \hline C_M & D \end{array} \right] \quad (A1)$$

The spectral factorization algorithm in Ref. 24 relies on finding the modal spaces $X_-(A_M^\times)$ and $X_+(A_M)$ corresponding to the left half plane zeros of M and the right half plane poles, respectively. Instead, now find $X_+(A_M^\times)$ and $X_+(A_M)$, corresponding to right half plane zeros and right half plane poles. If these two spaces are complementary, then the required factorization exists.

Since the unstable poles of any matrix A are the stable poles of $-A$,

$$X_+(A_M^\times) = X_-(-A_M^\times) \quad (A2)$$

Thus, the desired factorization exists if $X_-(-A_M^\times)$ and $X_+(A_M)$ are complementary.

Since A_M^\times is a Hamiltonian matrix, $-A_M^\times$ is as well. Thus, there exists a matrix

$$X_2 = \text{Ric}\{-A_M^\times\} \quad (A3)$$

such that

$$X_-(-A_M^\times) = \text{Im} \begin{bmatrix} I \\ X_2 \end{bmatrix} \quad (A4)$$

and this is complementary to $X_+(A_M)$. Given this, the remainder of the derivation follows Francis exactly, so that

$$G_1(s)G_0^-(s) = \left[\begin{array}{c|c} A & B_2 \\ \hline D^{-1/2}(C_2 + B_2^T X_2) & D^{1/2} \end{array} \right] \quad (A5)$$

Appendix B: Calculation of W_2

As noted earlier, the computation of the weighting function W_2 in Eq. (25) from W_1 can also be represented in terms of a spectral factorization. First, represent W_1 in state space as

$$W_1 = \left[\begin{array}{c|c} A_w & B_w \\ \hline C_w & D_w \end{array} \right] \quad (B1)$$

Then

$$W_1^- = \left[\begin{array}{c|c} -A_w^T & -C_w^T \\ \hline B_w^T & D_w^T \end{array} \right] \quad (B2)$$

Combining these gives

$$W_1 W_1^- = \left[\begin{array}{c|c} A_w & 0 \\ \hline -C_w^T C_w & -A_w^T \\ \hline -D_w^T C_w & -B_w^T \end{array} \middle| \begin{array}{c} B_w \\ -C_w^T D_w \\ -D_w^T D_w \end{array} \right] \quad (B3)$$

Define the similarity transformation

$$T = \begin{bmatrix} I & 0 \\ X_w & I \end{bmatrix} \quad (B4)$$

where X_w satisfies the Lyapunov equation

$$A_w^T X_w + X_w A_w + C_w^T C_w = 0 \quad (B5)$$

and use this to transform the system in Eq. (B3). This gives

$$W_1 W_1^- = \left[\begin{array}{c|c} A_w & 0 \\ \hline 0 & -A_w^T \\ \hline \tilde{C}_w & -B_w^T \end{array} \middle| \begin{array}{c} B_w \\ -\tilde{C}_w^T \\ -D_w^T D_w \end{array} \right] \quad (B6)$$

where

$$\tilde{C}_w = B_w^T X_w + D_w^T C_w \quad (B7)$$

Then W_2 is a spectral factor of

$$I - W_1 W_1^- = \left[\begin{array}{c|c} A_w & 0 \\ \hline 0 & -A_w^T \\ \hline -\tilde{C}_w & -B_w^T \end{array} \middle| \begin{array}{c} B_w \\ \tilde{C}_w^T \\ I - D_w^T D_w \end{array} \right] \quad (B8)$$

This is now in the form of a standard spectral factorization. In order to apply the algorithm, W_1 must satisfy

$$I - D_w^T D_w > 0 \quad (B9)$$

or $W_1(\infty) < 1$. This is not a limitation at all since multiplying the weighting function everywhere by a constant will not change the resulting compensator. The other conditions specified in the definition of the spectral factorization are also satisfied, provided W_1 has no imaginary poles. Note that, if $|W_1| < 1$ at all frequencies, then $I - W_1 W_1^-$ can have no imaginary zeros.

Acknowledgments

This work was supported by the Air Force Office of Scientific Research under Grant AFOSR-88-0029 with Anthony K. Amos serving as technical monitor. The authors wish to thank David Miller for many useful conversations and suggestions and K. Matsuda for pointing out an error in an earlier manuscript.

References

- ¹Balas, M. J., "Trends in Large Space Structure Control Theory: Fondest Hopes, Wildest Dreams," *IEEE Transactions on Automatic Control*, Vol. AC-27, No. 3, 1982, pp. 522-535.
- ²Doyle, J. C., and Stein, G., "Multivariable System Design: Concepts for a Classical/Modern Synthesis," *IEEE Transactions on Automatic Control*, Vol. AC-26, No. 1, 1981, pp. 4-16.
- ³Bernstein, D. S., and Hyland, D. C., "Optimal Projection for Uncertain Systems (OPUS): A Unified Theory of Reduced Order, Robust Control Design," *Large Space Structures: Dynamics and Control*, edited by S. N. Atluri and A. K. Amos, Springer-Verlag, New York, 1988, pp. 263-302.
- ⁴Doyle, J. C., "Analysis of Feedback Systems with Structured Uncertainties," *IEE Proceedings*, Vol. 129, Pt. D, No. 6, 1982, pp. 242-250.
- ⁵Miller, D. W., Hall, S. R., and von Flotow, A. H., "Optimal Control of Power Flow at Structural Junctions," *Journal of Sound and Vibration*, Vol. 140, No. 3, 1990, pp. 475-497.
- ⁶Miller, D. W., and Hall, S. R., "Experimental Results Using Active Control of Traveling Wave Power Flow," *Journal of Guidance, Control, and Dynamics*, Vol. 14, No. 2, pp. 350-359.
- ⁷Von Flotow, A. H., "The Acoustic Limit of Structural Dynamics," *Large Space Structures: Dynamics and Control*, edited by Atluri and Amos, Springer-Verlag, New York, 1988, pp. 213-238.
- ⁸Von Flotow, A. H., and Schäfer, B., "Wave-Absorbing Controllers for a Flexible Beam," *Journal of Guidance, Control, and Dynamics*, Vol. 9, No. 6, 1986, pp. 673-680.
- ⁹Mace, B. R., "Active Control of Flexural Vibrations," *Journal of Sound and Vibration*, Vol. 114, No. 2, 1987, pp. 253-270.

¹⁰Hagedorn, P., and Schmidt, J. T., "Active Vibration Damping of Flexible Structures Using the Travelling Wave Approach," *Proceedings of the Second International Symposium on Spacecraft Flight Dynamics*, Darmstadt, Germany, European Space Agency, Rept. SP-255, Oct. 1986, pp. 47-52.

¹¹Redman-White, W., Nelson, P. A., and Curtis, A. R. D., "Experiments on the Active Control of Flexural Wave Power Flow," *Journal of Sound and Vibration*, Vol. 112, No. 1, 1987, pp. 187-191.

¹²Scheuren, J., "Active Control of Bending Waves in Beams," *Proceedings of Internoise*, Wirtschaftsverband NW, D-Bremerhaven, Sept. 1985, pp. 591-594.

¹³Aubrun, J. N., "Theory of the Control of Structures by Low-Authority Controllers," *Journal of Guidance and Control*, Vol. 3, No. 5, 1980, pp. 444-451.

¹⁴MacMartin, D. G., "An H_∞ Power Flow Approach to Control of Uncertain Structures," S.M. Thesis, Department of Aeronautics and Astronautics, Massachusetts Inst. of Technology, Cambridge, MA, Feb. 1990.

¹⁵MacMartin, D. G., and Hall, S. R., "Structural Control Experiments Using an H_∞ Power Flow Approach," *Journal of Sound and Vibration* (to be published); also *Proceedings of the 1990 AIAA Guidance, Navigation, and Control Conference*, AIAA, Washington, DC, pp. 1634-1644.

¹⁶Lyon, R. H., *Machinery Noise and Diagnostics*, Butterworth, Boston, June 1987.

¹⁷Slater, G. L., Zhang, Q., and Bosse, A., "Robustness with Positive Real Controllers for Large Space Structures," *Proceedings of the*

1989 AIAA Guidance, Navigation, and Control Conference, Boston, MA, Aug. 1989, AIAA, Washington, DC, pp. 932-941.

¹⁸Hodges, C. H., and Woodhouse, J., "Theories of Noise and Vibration Transmission in Complex Structures," *Reports on Progress in Physics*, Vol. 49, 1986, pp. 107-170.

¹⁹Skudrzyk, E., "The Mean-Value Method of Predicting the Dynamic Response of Complex Vibrators," *Journal of the Acoustical Society of America*, Vol. 67, No. 4, 1980, pp. 1105-1135.

²⁰Bernstein, D. S., and Haddad, W. M., "LQG Control with an H_∞ Performance Bound: A Riccati Equation Approach," *IEEE Transactions on Automatic Control*, Vol. 34, No. 3, 1989, pp. 293-305.

²¹Miller, D. W., and von Flotow, A. H., "A Traveling Wave Approach to Power Flow in Structural Networks," *Journal of Sound and Vibration*, Vol. 128, No. 1, 1989, pp. 145-162.

²²Fuhrmann, P. A., "Elements of Factorization Theory From a Polynomial Point of View," *Three Decades of Mathematical System Theory*, edited by H. Nijmeijer and J. M. Schumacher, Springer-Verlag, New York, 1989, pp. 148-178.

²³Van Valkenburg, M. E., and Kinarwalla, B. K., *Linear Circuits*, Prentice-Hall, Englewood Cliffs, NJ, 1982, pp. 297-298.

²⁴Francis, B. A., *A Course in H_∞ Control Theory*, Springer-Verlag, New York, 1987.

²⁵Doyle, J. C., Glover, K., Khargonekar, P. P., and Francis, B. A., "State-Space Solutions to Standard H_2 and H_∞ Control Problems," *IEEE Transactions on Automatic Control*, Vol. 34, No. 8, 1989, pp. 831-847.

Recommended Reading from the AIAA

Progress in Astronautics and Aeronautics Series . . . 

Spacecraft Dielectric Material Properties and Spacecraft Charging

Arthur R. Frederickson, David B. Cotts, James A. Wall and Frank L. Bouquet, editors

This book treats a confluence of the disciplines of spacecraft charging, polymer chemistry, and radiation effects to help satellite designers choose dielectrics, especially polymers, that avoid charging problems. It proposes promising conductive polymer candidates, and indicates by example and by reference to the literature how the conductivity and radiation hardness of dielectrics in general can be tested. The field of semi-insulating polymers is beginning to blossom and provides most of the current information. The book surveys a great deal of literature on existing and potential polymers proposed for noncharging spacecraft applications. Some of the difficulties of accelerated testing are discussed, and suggestions for their resolution are made. The discussion includes extensive reference to the literature on conductivity measurements.

TO ORDER: Write, Phone or FAX:

American Institute of Aeronautics and Astronautics
c/o TASC0
9 Jay Gould Ct., P.O. Box 753, Waldorf, MD 20604
Phone (301) 645-5643, Dept. 415 • FAX (301) 843-0159

Sales Tax: CA residents, 7%; DC, 6%. For shipping and handling add \$4.75 for 1-4 books (call for rates for higher quantities). Orders under \$50.00 must be prepaid. Foreign orders must be prepaid. Please allow 4 weeks for delivery. Prices are subject to change without notice. Returns will be accepted within 15 days.

1986 96 pp., illus. Hardback
ISBN 0-930403-17-7
AIAA Members \$29.95
Nonmembers \$37.95
Order Number V-107